

## Connection between igneous activity and extension in the central Mojave metamorphic core complex, California

J. Douglas Walker,<sup>1</sup> John M. Fletcher,<sup>2,3</sup> Robert P. Fillmore,<sup>1,4</sup> Mark W. Martin,<sup>1,5</sup> Wanda J. Taylor,<sup>6</sup> Allen F. Glazner,<sup>7</sup> and John M. Bartley<sup>2</sup>

**Abstract.** The development of metamorphic core complexes and associated low-angle detachment faults commonly is intimately associated with synextensional igneous activity. In most areas studied to date, the relation of magmatism to extension is obscured by imprecise dating and by the overprint of later tectonic events. We present data from the early Miocene central Mojave metamorphic core complex (CMMCC) which indicate that extension was accompanied by igneous activity, as reflected by prekinematic, synkinematic, and postkinematic plutons and coeval volcanic rocks deposited in the associated extensional basins. The principal intrusion is an early Miocene granite pluton exposed in outcrops across an area greater than 400 km<sup>2</sup>. Dikes adjacent to the pluton are common in the Mitchel Range, at The Buttes, and at Fremont Peak. The overall orientation of the pluton and associated dikes is west-northwest, roughly perpendicular to the extension direction. Results of U-Pb analyses on zircon from two pluton and two dike samples yield ages of 20 to 23 Ma. Two other dike samples yield inconclusive results. Synextensional basins formed by detachment faulting during the core complex development. Rocks in these basins compose the Jackhammer and Pickhandle formations and filled an elongate, NW trending trough more than 50 km long. The <sup>40</sup>Ar/<sup>39</sup>Ar ages for tuff beds are as old as 23.8 ± 0.3 Ma near the base of the lower Pickhandle Formation and as young as 21.3 ± 0.5 Ma in the uppermost lower Pickhandle. Hence volcanism and plutonism are coeval. The diversity of intrusive relations relative to the timing and development of the mylonitic fabric in the CMMCC precludes any simple cause-and-effect relationship between magmatism and extensional deformation. Rather, magmatism and extension may have been localized at a releasing bend in a transfer-fault system which links extension in the CMMCC with extension in the Colorado River area to the east.

### Introduction

For the last 15 years, it has become widely recognized that large-magnitude extension in Cordilleran metamorphic core complexes is commonly associated with synkinematic igneous activity [Anderson *et al.*, 1988; Coney, 1980; Crittenden, 1980; Reynolds and Rehrig, 1980]. Synkinematic intrusions have been used to determine the timing and depth of mylonitic deformation [Anderson *et al.*, 1988; Reynolds *et al.*, 1986]. Some recent interpretations attribute much of the mylonitic deformation and patterns of cooling ages within core complexes to synextensional intrusion [e.g., Lister and Baldwin, 1993].

The evolution of detachment fault systems in metamorphic core complexes has also been interpreted using the record of synextensional sedimentary basins [Beratan, 1991; Dickinson, 1991; Duebendorfer and Wallin, 1991; Fedo and Miller, 1992; Nielson and Beratan, 1990]. Facies variations in the basins can be used to interpret the position of concealed faults and lateral changes in displacement in the detachment system. Dating of volcanic rocks in the rift sequence provides further controls on the temporal and spatial evolution of crustal extension in the area.

This paper examines the timing of igneous activity and basin formation relative to deformation within a core complex setting: We present geochronologic data from the central Mojave Desert metamorphic core complex (CMMCC), California which demonstrate synchronicity between igneous activity, basin formation, and footwall ductile deformation. The central Mojave Desert experienced large-magnitude extension in early Miocene time [Dokka *et al.*, 1988; Glazner *et al.*, 1988, 1989; Martin *et al.*, 1993; Walker *et al.*, 1990] and extension was associated with synkinematic intrusion of both dikes and a large granite pluton [Glazner *et al.*, 1992; Walker *et al.*, 1990]. In addition, a suite of sedimentary basins, filled in part with volcanic and volcanogenic rocks, developed in the area of extension [Dokka *et al.*, 1988; Fillmore and Walker, 1993, 1995; Walker *et al.*, 1990]. We review the geologic setting of the CMMCC, followed by age data for both intrusive and extrusive rocks, focusing on the important field relationships that define the nature of (1) the interplay between plutonism and ductile deformation, (2) the temporal and spatial evolution of the detachment fault system, and (3) structure of the extended terrane. Our data show that mylonitization, plu-

<sup>1</sup>Isotope Geochemistry Laboratory and Department of Geology, University of Kansas, Lawrence.

<sup>2</sup>Department of Geology and Geophysics, University of Utah, Salt Lake City.

<sup>3</sup>Now at Departamento de Geología, Centro de Investigación Científica y Educación Superior de Ensenada, Ensenada, Baja California, Mexico.

<sup>4</sup>Now at Department of Geology, Northern Arizona University, Flagstaff.

<sup>5</sup>Now at Servicio Nacional de Geología y Minería-Chile, Santiago, Chile.

<sup>6</sup>Department of Geoscience, University of Nevada, Las Vegas.

<sup>7</sup>Department of Geology, University of North Carolina, Chapel Hill.

Copyright 1995 by the American Geophysical Union.

Paper number 94JB03132.  
0148-0227/95/94JB-03132\$05.00

tonism, and basin development were roughly coeval and intimately connected. We then speculate about the overall connections between intrusion and extensional deformation.

## Geologic Setting

The study area encompasses a belt of northeast directed, metamorphic core complex-style extension in the central Mojave Desert (Figure 1). Mylonitic footwall rocks are exposed widely in the Waterman Hills, Mitchel Range, Hinkley Hills, and The Buttes and collectively constitute the central Mojave metamorphic core complex [Bartley *et al.*, 1990]. Footwall rocks are separated from hanging wall rocks by the Waterman Hills detachment fault. This structure apparently evolved as a ductile/brittle detachment during the early Miocene [Glazner *et al.*, 1988, 1989; Bartley *et al.*, 1990; Fletcher, 1994]. A northwest trending belt of Miocene dikes and plutons that extends from the Mitchel Range to Fremont Peak spatially coincides with footwall rocks of the CMMCC [Fletcher and Bartley, 1994; Bartley *et al.*, 1990]. Mylonitic rocks are always found in close proximity to Miocene intrusions, but the intrusions occur in a broader region that includes portions of the hanging wall (e.g., Lead Mountain) and areas that show little to no evidence for mylonitization (e.g., Fremont Peak).

Miocene granitic rocks crop out in three main areas in the CMMCC: the Waterman Hills, northern Lynx Cat Mountain, and The Buttes (Figure 1). The granitic rocks probably form a continuous batholith at depth which we refer to as the Waterman Hills granite (WHG). Outcrops of the WHG occur over an area of 400 km<sup>2</sup>. The WHG is a medium-grained, equigranular granite containing plagioclase, orthoclase, quartz, biotite, rare hornblende, and allanite. Miocene dikes are exposed from the Mitchel Range northwestward to Fremont Peak (Figure 1). Porphyritic dacite is the dominant rock type of the Miocene dikes, but felsite and basalt dikes also are common.

It is clear that the WHG and dikes were emplaced roughly synkinematically with the extensional mylonitization. Mylonitization in the WHG commonly intensifies from undeformed and protomylonitic at deeper structural levels to ultramylonitic near the brittle detachment [e.g., Bartley *et al.*, 1990; Fletcher and Bartley, 1994]. Wall rock/pluton contacts generally are poorly exposed in the CMMCC. These relationships are best exposed in the Waterman Hills and Mitchel Range, and the wall rocks record far higher strain magnitudes than the WHG. Either there is a large strain gradient between the wall rocks and the WHG or the granite was emplaced synkinematically and records only the later stages of deformation. Fletcher and Bartley [1994] favor the latter idea because strain analysis of pre-Tertiary wall rock granites of similar composition and mineralogy (and hence rheology) to the Miocene WHG show much higher mylonitic strains in the older rock. Also in the Mitchel Range, there is generally no difference between the degree of mylonitization in the dacite dikes and their wall rocks, suggesting that the dikes were emplaced before or early in the deformational history. Given that the dikes and WHG are approximately the same age (see below), this indicates a broadly synkinematic relation between intrusion and mylonitization in the Waterman Hills and Mitchel Range.

The clearest example of synkinematic intrusion of Miocene dikes is in the Hinkley Hills [Fletcher, 1994]. Dikes completely postdate mylonitization in the footwall of the detachment, except for dikes in the easternmost exposure, which do contain the mylonitic fabric. However, all dikes are crosscut by the brittle detachment, suggesting that they were emplaced during active dis-

placement across the brittle/ductile detachment system. In The Buttes, mylonitization is concentrated into discrete shear zones that show mutual cross-cutting relationships with the dacite dikes: shear zones cut some of the dikes but are in turn cut by undeformed dikes [Fletcher, 1994]. For example, dike sample Buttes-51 (see below) contains a mylonitic shear zone: both the sampled dike and the shear zone are cut by an identical but wholly undeformed dike. In some cases, dacite dikes in The Buttes contain a wall-parallel mylonitic fabric that only affects the country rock within 0.1-1.0 m of the contact. The highly localized mylonitization may reflect a thermal anomaly associated with the dike emplacement. This indicates to us that deformation and intrusion were broadly coeval.

In summary, dikes and plutons of demonstrably similar ages (see below) display prekinematic, synkinematic, and postkinematic relations to the extension-related mylonitic fabric in the CMMCC. This indicates that mylonitization and plutonism were coeval. In addition, despite the close spatial association of plutonism and mylonitization, there is no single temporal sequence relating the two throughout the CMMCC. (See Bartley *et al.* [1990] and Fletcher and Bartley [1994] for further information about the nature of the ductile fabrics.)

The only previously published zircon U-Pb age of Miocene intrusive rocks in the CMMCC was on a dacite dike in the footwall of the CMMCC in the Mitchel Range, which yielded an age of  $23 \pm 0.9$  Ma [Walker *et al.*, 1990]. Thermochronologic studies show pronounced cooling at  $\sim 19$  Ma [Dokka and Baksi, 1988]. Hence the metamorphic core experienced deformation, intrusion, and subsequent cooling over a short interval starting in latest Oligocene or earliest Miocene time.

Synextensional strata related to development of the CMMCC are exposed in the hanging wall of the detachment system and include the Jackhammer and Pickhandle formations [Dibblee, 1967, 1968; McCulloh, 1952, 1960]. The overlying Barstow Formation represents postextensional basin fill [Dokka, 1989; Walker *et al.*, 1990; Fillmore and Walker, 1995]. Discussion of stratigraphy in this paper is restricted to the Jackhammer and Pickhandle formations (shown as Pickhandle Group on Figure 1).

The Jackhammer Formation lies nonconformably on pre-Tertiary plutonic basement rocks. At its type locality at Jackhammer Pass, located between the Mud Hills and the Calico Mountains (Figure 1), the formation comprises  $\sim 200$  m of sandstone, conglomerate, tuff, and basalt [McCulloh, 1952]. In the Mud Hills to the west and at Lead Mountain to the south the Jackhammer thins considerably and is dominated by conglomerate and tuff. Elsewhere it is absent. The age of the Jackhammer Formation is uncertain, but an apparently conformable relationship with the overlying Pickhandle Formation suggests that the Jackhammer is only slightly older. For the purposes of this paper it is grouped with the lower Miocene Pickhandle Formation.

The Pickhandle Formation ranges to more than 1000 m thick and consists of a heterogeneous succession of pyroclastic and epiclastic volcanic rocks, megabreccia, conglomerate, sandstone, siltstone, and carbonate. The formation constitutes a northwest trending outcrop belt and is well exposed in the Gravel Hills, Mud Hills, Waterman Hills, Calico Mountains, and Lead Mountain (Figure 1). At Lead Mountain, the Calico Mountains, and the Mud Hills the Pickhandle Formation rests on the Jackhammer Formation. Elsewhere it lies nonconformably on pre-Tertiary plutonic rocks or in fault contact with footwall rocks of the CMMCC.

The Pickhandle can be divided into upper and lower members based on overall compositional and depositional characteristics:

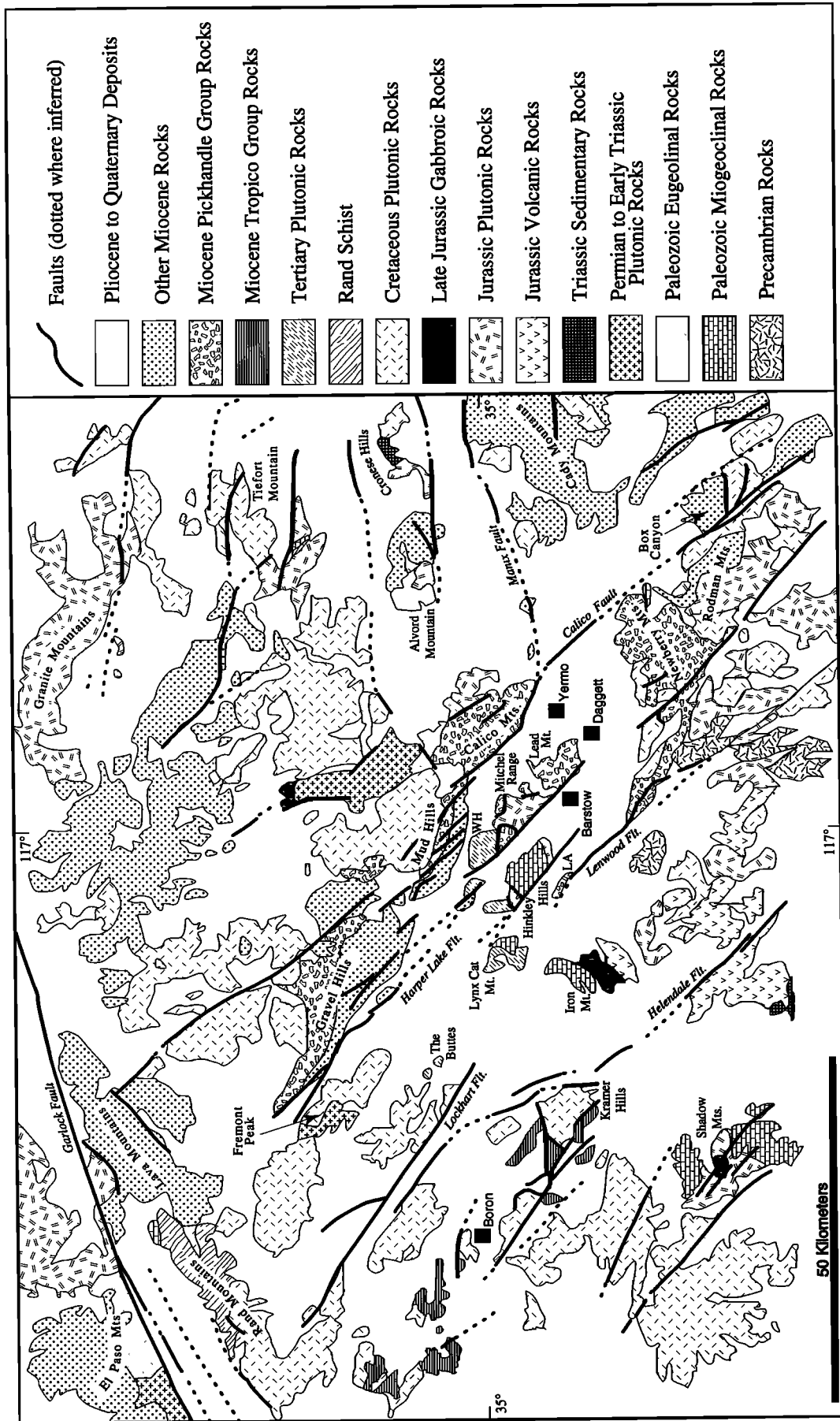


**Figure 1.** Generalized geologic map of the central Mojave Desert region. The central Mojave metamorphic core complex comprises the area from The Buttes and Fremont Peak southeastward to Lead Mountain. The Waterman Hills detachment fault, the main low-angle normal fault in the CMMCC, is shown by bold lines bounding the upper plate Pickhandle Formation north of Barstow. LA, Lenwood anticline; WH, Waterman Hills. Compiled from Dibblee [1967, 1968].

the lower Pickhandle contains mainly volcanic and volcanogenic rocks, whereas the upper Pickhandle (Mud Hills Formation of [Dokka *et al.*, 1991]) is mainly plutoclastic in composition. Several previous studies have dated volcanic rocks that cap the upper Pickhandle Formation and provide a minimum age of crustal extension in the CMMCC. In the Gravel Hills, Burke *et al.* [1982] reported a K-Ar age of  $18.9 \pm 1.3$  Ma from the Opal Mountain Volcanic Member of the uppermost Pickhandle Formation. In the Mud Hills, megabreccia at the top of the Pickhandle interfingers with the Owl Canyon Member of the overlying Barstow Formation [Woodburne *et al.*, 1990]. The Red Tuff at the base of the Owl Canyon Member has yielded an  $^{40}\text{Ar}/^{39}\text{Ar}$  age of  $19.3 \pm 0.02$  Ma [MacFadden *et al.*, 1990; Woodburne *et al.*, 1990].

Other previous geochronologic work in the CMMCC includes the dating of several intrusive phases that cut synextensional sediments at Lead Mountain. Dokka and Woodburne [1986] report a  $25.6 \pm 0.8$  Ma age (K-Ar) for a basaltic sill that intruded between the Jackhammer Formation and their "formation of Lead Mountain." Similarly, Lambert *et al.* [1987] published a  $25.6 \pm 0.8$  Ma age (K-Ar) but for a felsite dike that cuts the Jackhammer Formation at Lead Mountain. Finally, Dokka *et al.* [1991] reported a whole rock  $^{40}\text{Ar}/^{39}\text{Ar}$  age of  $21.0 \pm 0.8$  Ma from a felsite dike that cuts their Jackhammer Formation. These ages should indicate the minimum age of the strata at Lead Mountain, but no locations or analytical data have been published. As discussed below, the new data presented in this paper do not agree with some of these reported ages.

This paper presents a more complete geochronologic data set for the CMMCC which allows regional chronologic correlations of intrusive phases and synextensional strata. The data also demonstrate the tight range of ages for the plutonic rocks of the CMMCC. Last, we discuss the connection of basin formation to intrusion and extensional faulting, and the relation between mylonitization and plutonism.

## Geochronology

This section presents data and interpretations for the crystallization and cooling ages of plutonic and volcanic units around the CMMCC. In all, results from six U-Pb zircon and thirteen  $^{40}\text{Ar}/^{39}\text{Ar}$  samples are reported (Tables 1-3 and Table A1<sup>1</sup>).

### U-Pb Methods

Samples were crushed and zircon/heavy mineral separates were isolated by standard density/magnetic susceptibility techniques at the University of Kansas. All samples analyzed were hand picked to 100% purity. Isotopic analyses were determined on a VG Sector multicollector thermal ionization mass spectrometer at the University of Kansas. Further information about the chemical procedures, zircon characteristics, and decay constants are given in Table 2.

<sup>1</sup>An electronic supplement of this material may be obtained on a diskette or Anonymous FTP from KOSMOS.AGU.ORG. (LOGIN to AGU's FTP account using ANONYMOUS as the username and GUEST as the password. Go to the right directory by typing CD APEND. Type LS to see what files are available. Type GET and the name of the file to get it. Finally, type EXIT to leave the system.) (Paper 94JB03132, Connection between igneous activity and extension in the central Mojave metamorphic core complex, California, by J. D. Walker, J. M. Fletcher, R. P. Fillmore, M. W. Martin, W. J. Taylor, A. F. Glazner, and J. M. Bartley). Diskette may be ordered from American Geophysical Union, 2000 Florida Avenue, N.W., Washington, DC 20009; \$15.00. Payment must accompany order.

### The $^{40}\text{Ar}/^{39}\text{Ar}$ Methods

Samples were crushed and sieved to uniform grain sizes and a size range was selected that yielded the largest possible individual (not composite) grains. Standard physical methods (magnetic/density techniques and hand picking) were used to extract mineral separates of biotite, sanidine, hornblende, and plagioclase with an estimated purity of >99.9%. The physical separations were variably performed at mineral separation facilities at the universities of Utah, North Carolina, Nevada at Las Vegas, and Kansas.

Some of the samples for  $^{40}\text{Ar}/^{39}\text{Ar}$  dating were analyzed at Cambridge Laboratory for Argon Isotopic Research (CLAIR) at the Massachusetts Institute of Technology and some at the University of Maine. A summary of methods for each laboratory is given below. Mineral separates were analyzed using the incremental heating technique.

Samples analyzed at Maine were irradiated in the nuclear reactor at the Phoenix Memorial Laboratory at the University of Michigan. An intralaboratory standard, SBG-7, calibrated to hornblende standard MMhb-1 [Alexander *et al.*, 1978], was used as an irradiation monitor. Irradiation packages included neutron flux monitors at the top and bottom of each vial and every one or two samples. Methods of isotope measurements and data reduction are described by Hubacher and Lux [1987].

Samples analyzed at CLAIR were irradiated at the McMaster Research Facility, Ontario, Canada, with Cd shielding. Corrections for interfering reactions on Ca, K, and Cl were based on analyses of  $\text{CaF}_2$ ,  $\text{K}_2\text{SO}_4$ , and KCl included in the irradiation package. Fast neutron flux was monitored using MMhb-1 hornblende [Alexander *et al.*, 1978; Samson and Alexander, 1987] and Fish Canyon sanidine [Cebula *et al.*, 1986]. Methods of isotope measurements and data reduction are described by Hodges *et al.* [1994].

### U-Pb Results

Most of the Miocene intrusive phases in the footwall of the CMMCC were dated by U-Pb on zircon (Table 2 and Figure 2). We have dated two exposures of the WHG. The four other samples come from exposures of Miocene dikes in the CMMCC.

**Sample BAR9020A.** This is a sample of WHG collected at Lynx Cat Mountain (Figure 1). Six fractions were analyzed. All fractions are discordant and mostly show evidence of complex inherited, xenocrystic zircon and/or Pb loss. A discord through these data gives a lower intercept of  $20 \pm 4$  Ma and a poorly defined Proterozoic upper intercept (Figure 2a).

**Sample Buttes-50.** This sample of WHG in The Buttes came from an isolated hill that is relatively undeformed at the base but becomes mylonitic upward over a vertical distance of 30 to 40 m. The behavior of zircons from this sample (Figure 2b) is similar to those in sample BAR9020A. This sample yields a lower intercept age of  $22.0 \pm 3.8$  Ma, and an upper Proterozoic upper intercept age.

**Sample Buttes-51.** This sample comes from a dacite porphyry dike cut by a mylonitic shear zone. Importantly, the sample came from the nonmylonitic portion of the dike exposure. These zircons show evidence for minor inheritance of xenocrystic zircons and minor Pb loss (Figure 2c). One fraction is concordant and another nearly so at 21.9 Ma. A discord through these points yields a lower intercept age of  $21.9 \pm 1.4$  Ma.

**Sample FP-1.** These data are on a dike from the Fremont Peak area. None of the fractions were concordant, and the data form an array parallel to concordia (Figure 2d). This appears to

**Table 1. Sample Locations and Descriptions**

Sample	Location	Description
<sup>40</sup> Ar/ <sup>39</sup> Ar samples		
GH-52 Plagioclase	35°13'0" N, 117°21'52"W	Massive white, feldspar hornblende biotite tuff in lower Pickhandle Formation in Gravel Hills 15.3 m above basal contact with granitic basement. Tuff bed is 2.4 m thick.
LM-37 Biotite	34°55'37"N, 116°55'44"W	Purple and tan pumiceous biotite tuff in lower Pickhandle Formation at Lead Mountain. The tuff unit is 22.7 m thick and located 17.6 m from the base of a partial section in which the base of the formation was not exposed.
LM-38 Biotite	34°55'37"N, 116°55'44"W	White biotite tuff in the middle to upper Pickhandle Formation at Lead Mountain. Tuff unit is 0.9 m thick and is 48.7 m above the base of a partial section in which the base of the formation is not exposed.
MH92-1 K-Spar	35°02'34"N, 117°00'22"W	Dacite block and ash flow unit in lower Pickhandle Formation from the exposed base in Mud Hills. The unit is 2.1 m thick and consists of pebble-sized clasts of brown biotite feldspar dacite in a brown biotite crystal tuff matrix.
MH92-2 Biotite	35°02'23"N, 117°00'20"W	Brown crystal tuff unit in middle Pickhandle Formation in Mud Hills 141.6 m from the exposed base of the formation. The unit is 50 m thick and contains abundant feldspar and euhedral biotite phenocrysts.
MH92-3 Biotite	35°02'23"N, 117°00'13"W	Red and white feldspar biotite tuff in middle Pickhandle Formation in Mud Hills. The unit is 191.6 m from the exposed base of the formation and is 1.8 m thick.
WH-10 Biotite	34°57'40"N, 117°02'15"W	Pumiceous pink tuff with abundant biotite pumice clasts in middle Pickhandle Formation in Waterman Hills. The unit is 19.7 m thick.
WHG-14 Biotite	34°50'01"N, 117°02'13"W	Massive cliff exposure of red biotite-plagioclase-quartz rhyolite plug immediately south of microwave towers in the Waterman Hills.
BAR9020A Biotite	34°59'05"N, 117°14'32"W	Fresh biotite granite with no discernible fabric from already broken rock in quarry on west side of Lynx Cat Mountain.
GD-1 Biotite	35°00'13"N, 117°02'58"W	Weakly tectonized Waterman Hills granite from northern Waterman Hills.
BARS-B Biotite	34°52'39"N, 117°05'49"W	Massive layer, several meters thick, of friable white tuff exposed along powerline road near Lenwood. Layering in tuff nearby shows evidence of reworking, but this layer appears to be a pyroclastic fall deposit with little reworking.
ROD3.19 Plagioclase	34°41'32"N, 116°30'41"W	Lithic airfall tuff bed interbedded in conglomerate exposed on the western wall of Silver Bell Canyon, Rodman Mountains. Contacts of the tuff bed are poorly exposed, but the bed is estimated to be 3 m thick. The tuff contains abundant volcanic lithic fragments and phenocrysts of plagioclase and altered biotite and hornblende. Xenocrystic contamination of the separate is deemed unlikely based on microprobe analysis of several grains from the separate which yielded a composition of An <sub>35±0.6</sub> ; such compositional uniformity strongly suggests a single origin. The precise stratigraphic position of the sample is uncertain because of local structural complexities but is no more than 100 m above the base of the conglomerate, which overlies a sequence of nearly 2 km of intermediate to mafic lava flows of probable early Miocene age.
BOXC-26 Biotite	34°41'13"N, 116°31'30"W	Light pink plagioclase-biotite tuff taken about 150 m upstream of Silver Bell fault; immediately overlain by breccia of biotite quartz monzonite.
U-Pb zircon samples		
BAR9020A Buttes-50	35°03'57"N, 117°23'33"E	(see above) Medium-grained, light gray, biotite granite. Collected at the undeformed base of a prominent tor which shows a gradient in fabric intensity contains well-developed mylonites on its summit. No pluton/wallrock relationships exposed in The Buttes. Since the granite contains the mylonitic fabric, it was emplaced either synkinematically or prekinematically.
Buttes-51	35°05'16"N, 117°25'06"E	Porphyritic dacite dike characterized by plagioclase and biotite phenocrysts and a yellowish-brown aphanitic matrix. Sample was collected from the undeformed southern portion of the dike. Northern portion of dike is crosscut by a mylonitic shear zone as well as another dacite dike which is unmylonitized. The dated dike was emplaced prekinematically and the cross cutting dike was emplaced postkinematically.
FP-1	35°13'04"N, 117°30'16"W	Porphyritic dacite dike characterized by feldspar and minor biotite phenocrysts in an aphanitic, orange weathering matrix. The dike is 1 to 2 m thick and surrounded by alluvium. No mylonitic fabrics are apparent.
HH-1	34°56'12"N, 117°06'06"W	Undeformed dacite porphyry dikes with feldspar and minor biotite phenocrysts in an aphanitic groundmass.
HH-16	34°54'17"N, 117°04'46"W	Undeformed dacite porphyry dikes with feldspar and minor biotite phenocrysts in an aphanitic groundmass.

Table 2. Analytic Data for Barstow Area Samples

Fraction	Sample Weight, mg	U, ppm	Pb, ppm	$^{206}\text{Pb}/^{204}\text{Pb} \ddagger$	Radiogenic Ratios†				Ages (Ma)		Common Pb, pg§			
					$^{206}\text{Pb}^*/^{238}\text{U}$	Percent Error	$^{207}\text{Pb}^*/^{235}\text{U}$	Percent Error	$^{206}\text{Pb}^*/^{238}\text{U}$	$^{207}\text{Pb}^*/^{235}\text{U}$		$^{207}\text{Pb}^*/^{206}\text{Pb}^*$	$^{206}\text{Pb}^*/^{206}\text{Pb}^*$	
					<i>BAR9020A</i>									
nm(1)<240	0.0190	1506	19.5	1060	0.01252	(1.14)	0.1248	(2.55)	0.07228	(2.12)	80.2	119.4	994	22
nm(0)eq	0.1270	366.1	3.2	427.5	0.008621	(2.26)	0.07772	(2.35)	0.06538	(0.60)	55.3	76.0	787	62
nm(0)<240	0.0960	480.1	3.3	379.9	0.006967	(2.34)	0.07362	(2.79)	0.07663	(1.50)	44.8	72.1	1112	57
m(0)>240	0.2790	979.4	4.1	612.0	0.004306	(0.78)	0.03360	(0.83)	0.05660	(0.27)	27.7	33.6	476	126
nm(0)>240eu	0.4010	1310	4.7	671.6	0.003713	(0.59)	0.02606	(0.77)	0.05092	(0.47)	23.9	26.1	237	191
nm(0) acic	0.0820	1013	3.5	196.1	0.003424	(2.50)	0.02295	(3.15)	0.04861	(1.79)	22.0	23.0	129	102
					<i>FP-1</i>									
nm(2)<100	0.0540	2594	9.0	1505	0.003408	(0.78)	0.02206	(0.86)	0.04694	(0.33)	21.9	22.2	46.4	20
nm(2)<100eu	0.1980	2715	9.6	557.2	0.003487	(0.53)	0.02255	(0.55)	0.04689	(0.17)	22.4	22.6	43.8	222
nm(3)<100eu	0.2590	2836	10.4	499.1	0.003621	(0.48)	0.02343	(0.51)	0.04693	(0.18)	23.3	23.5	45.7	354
nm(1)<100eu	0.1650	2460	8.8	183.3	0.003537	(0.50)	0.02295	(0.71)	0.04705	(0.49)	22.8	23.0	51.7	557
					<i>Buttes-51</i>									
nm(0)<240	0.428	1635	5.7	2462	0.003528	(0.48)	0.02299	(0.50)	0.04727	(0.13)	22.7	23.1	63.0	45
nm(1)<240	0.701	1894	6.4	2216	0.003397	(0.47)	0.02169	(0.50)	0.04632	(0.16)	21.9	21.8	14.3	94
nm(0)>240	0.497	1714	5.8	1601	0.003443	(0.48)	0.02256	(0.52)	0.04751	(0.18)	22.2	22.6	75.0	84
nm(1)<240aa	0.316	1837	6.1	2090	0.003383	(0.54)	0.02150	(0.75)	0.04609	(0.51)	21.8	21.6	2.50	45
nm(0)<240aa	0.669	1636	5.7	2679	0.003530	(0.48)	0.02305	(0.63)	0.04736	(0.40)	22.7	23.1	67.6	68
					<i>Buttes-50</i>									
nm(0)<200	0.048	1353	9.4	1490	0.007114	(0.79)	0.06398	(0.82)	0.06522	(0.21)	45.7	63.0	782	20
nm(1)<200eu	0.197	2578	10.5	532.4	0.004070	(0.53)	0.02843	(0.62)	0.05065	(0.31)	26.2	28.5	225	181
nm(1)<200	0.774	2980	14.2	1068	0.004725	(0.47)	0.03782	(0.51)	0.05805	(0.18)	30.4	37.7	531	450
nm(0)<200	3.097	2154	10.5	2494	0.004985	(1.09)	0.04023	(1.10)	0.05853	(0.10)	32.1	40.0	550	600
nm(-1)>200	1.178	1768	10.3	2946	0.005887	(0.51)	0.04923	(0.52)	0.06066	(0.08)	37.8	48.8	627	290
					<i>HH-1</i>									
nm(-1)<240	0.705	698.2	7.1	4300	0.009962	(0.46)	0.09868	(0.48)	0.07185	(0.10)	63.9	95.6	982	47
nm(0)<240	0.745	780.1	6.4	1123	0.007683	(0.47)	0.07105	(0.50)	0.06707	(0.17)	49.3	69.7	840	190
nm(-1)>240	1.041	491.6	6.9	2049	0.013492	(0.47)	0.1262	(0.50)	0.06782	(0.17)	86.4	120.6	863	150
nm(-1)>240eu	0.099	559.8	5.4	351.8	0.008005	(0.56)	0.05760	(0.60)	0.05219	(0.21)	51.4	56.9	294	85
nm(0)<240eu	0.060	795.4	4.8	1030	0.005639	(0.71)	0.04556	(0.75)	0.05861	(0.22)	36.2	45.2	553	17
					<i>HH-16</i>									
nm(-2)<100eu	0.060	627.7	6.6	871.5	0.009747	(0.93)	0.07848	(0.97)	0.05839	(0.25)	62.5	76.7	544	27
nm(-1)<100eu	0.196	684.0	4.9	1405	0.006842	(0.66)	0.05522	(0.68)	0.05882	(0.13)	43.7	54.6	560	42
nm(0)<100eu	0.127	813.6	7.4	5867	0.009022	(0.48)	0.08354	(0.49)	0.06716	(0.07)	57.9	81.5	843	10
nm(1)<100eu	0.218	819.0	4.5	5614	0.005504	(0.48)	0.03647	(0.50)	0.04806	(0.15)	35.4	36.4	102	11
>100	0.697	257.6	2.6	1522	0.009591	(0.61)	0.06657	(0.88)	0.05034	(0.62)	61.5	65.4	211	73

nm(#), nonmagnetic on Frantz separator at angle of tilt, number, degrees; m(#), magnetic on Frantz separator at angle of tilt, number, degrees; >240, size in standard mesh; aa, air abraded fraction; eu, euhedral fraction; acic, acicular grain fraction; eq, equant grain fraction. Zircon dissolution followed the methods of Krogh [1973] and Parrish [1987]. Elemental separation was done with a HBr anion column chemistry for lead and HCl column chemistry for uranium. Air abrasion followed the methods of Krogh [1982]. Decay constants used were  $^{238}\text{U}=0.15513 \times 10^{-9} \text{ yr}^{-1}$  and  $^{235}\text{U}=0.98485 \times 10^{-9} \text{ yr}^{-1}$  [Steiger and Jäger, 1977].

**Table 2.** (continued)

Isotopic analyses were determined on a VG Sector multicollector thermal ionization mass spectrometer. A mass fractionation correction of  $0.10\% \pm 0.05\% / \text{amu}$ , as determined by standard runs on NBS 981 (common lead) and NBS 982 (equal atom lead), was applied to the lead data. Samples were spiked with a mixed  $^{205}\text{Pb}/^{233}\text{U}$  spike or a mixed  $^{208}\text{Pb}/^{235}\text{U}$  spike. Errors on  $^{206}\text{Pb}/^{204}\text{Pb}$  were minimized by use of a Daly multiplier and are typically of the order of 1% or less. Errors for  $^{206}\text{Pb}/^{204}\text{Pb}$  were reduced further on samples spiked with  $^{208}\text{Pb}$  by using a dynamic Daly calibration after the technique of *Roddick et al.* [1987, p. 115]. Common lead corrections were made using values determined from Stacey and Kramers [1975] for 23 Ma.

\* Radiogenic component.

† Errors were computed using the method of Ludwig (1980).

‡ Ratio corrected for spike and mass fractionation only.

§ Total common Pb (blank and common) in the analysis.

**Table 3.** Summary of Ages

Sample	Mineral	Plateau Age, Ma	$^{39}\text{Ar}_p$ , %	Isochron or Concordia Intercept Age, Ma	$^{39}\text{Ar}_p$ , %	$(^{40}\text{Ar}/^{36}\text{Ar})_0$	MSWD	Field Relation
BAR9020A	Zr	—	—	20 ± 4	100	287 ± 8.4	4.8	undeformed Waterman Hills Granite
Buttes-50	Zr	—	—	22.0 ± 3.8	95	670 ± 410	280	undeformed Waterman Hills Granite
Buttes-51	Zr	—	—	21.9 ± 1.4	86	550 ± 210	27	undeformed portion of deformed dacite dike
FP-1	Zr	—	—	23 minimum	96	311 ± 70		undeformed dacite dike
HH-1	Zr	—	—	uncertain	93	350 ± 80		undeformed dacite dike
HH-16	Zr	—	—	uncertain	97	500 ± 400		undeformed dacite dike
MH92-1	Plag	—	—	22.4 ± 0.4	100	287 ± 8.4	0.1	basal Pickhandle Formation
MH92-2	Bt	—	—	21.7 ± 0.5	95	670 ± 410	2.1	upper part of lower Pickhandle
MH92-3	Bt	—	—	21.4 ± 0.5	86	550 ± 210	0.7	upper part of lower Pickhandle
GH-52	Plag	—	—	23.8 ± 0.5	98	325 ± 150	0.2	basal Pickhandle Formation
WH-10	Bt	21.7 ± 0.2	76	21.7 ± 0.5	96	311 ± 70	0.2	upper part of lower Pickhandle
LM-37	Bt	—	—	23.0 ± 0.5	93	350 ± 80	0.8	lower Pickhandle Formation
LM-38	Bt	23.6 ± 0.2	67	21.3 ± 0.5	97	500 ± 400	0.1	upper (?) part of lower Pickhandle
BOXC-26	Bt	24.0 ± 0.4	100	24.4 ± 0.3	100	295 ± 6	2.6	lower part of Box Canyon Sequence
ROD3.19	Plag	—	—	23.1 ± 0.6	100	320 ± 10	2.5	lower part of Rodman Sequence
BARS-B	Bt	—	—	21.8 ± 0.5	100	349 ± 35	2.8	tuff from Lenwood Anticline
WHG-14	Bt	—	—	20.0 ± 0.3	100	249 ± 5	2.6	rhyolite plug cutting Pickhandle
BAR9020A	Bt	20.2 ± 0.4	54	20.1 ± 0.2	100	302 ± 5	2.5	undeformed Waterman Hills Granite
GID-1	Bt	—	—	20.9 ± 0.3	100	247 ± 12	2.8	weakly deformed Waterman Hills Granite

For each sample, our interpretation of the best apparent age is the isochron or concordia intercept age. Zr, Zircon; Plag, Plagioclase; and Bt, Biotite. Data reduction and age interpretation techniques are given by *Hubacher and Lux* [1987] and *Hodges et al.* [1994]. The percentage  $^{39}\text{Ar}$  of the total  $^{39}\text{Ar}$  in the sample that was released in the heating steps included in the plateau are shown. The  $^{39}\text{Ar}_i$  column shows the percentage of total  $^{39}\text{Ar}$  in the heating steps used for the regression. All uncertainties are quoted at the  $2\sigma$  confidence level. MSWD, mean square of weighted deviates.

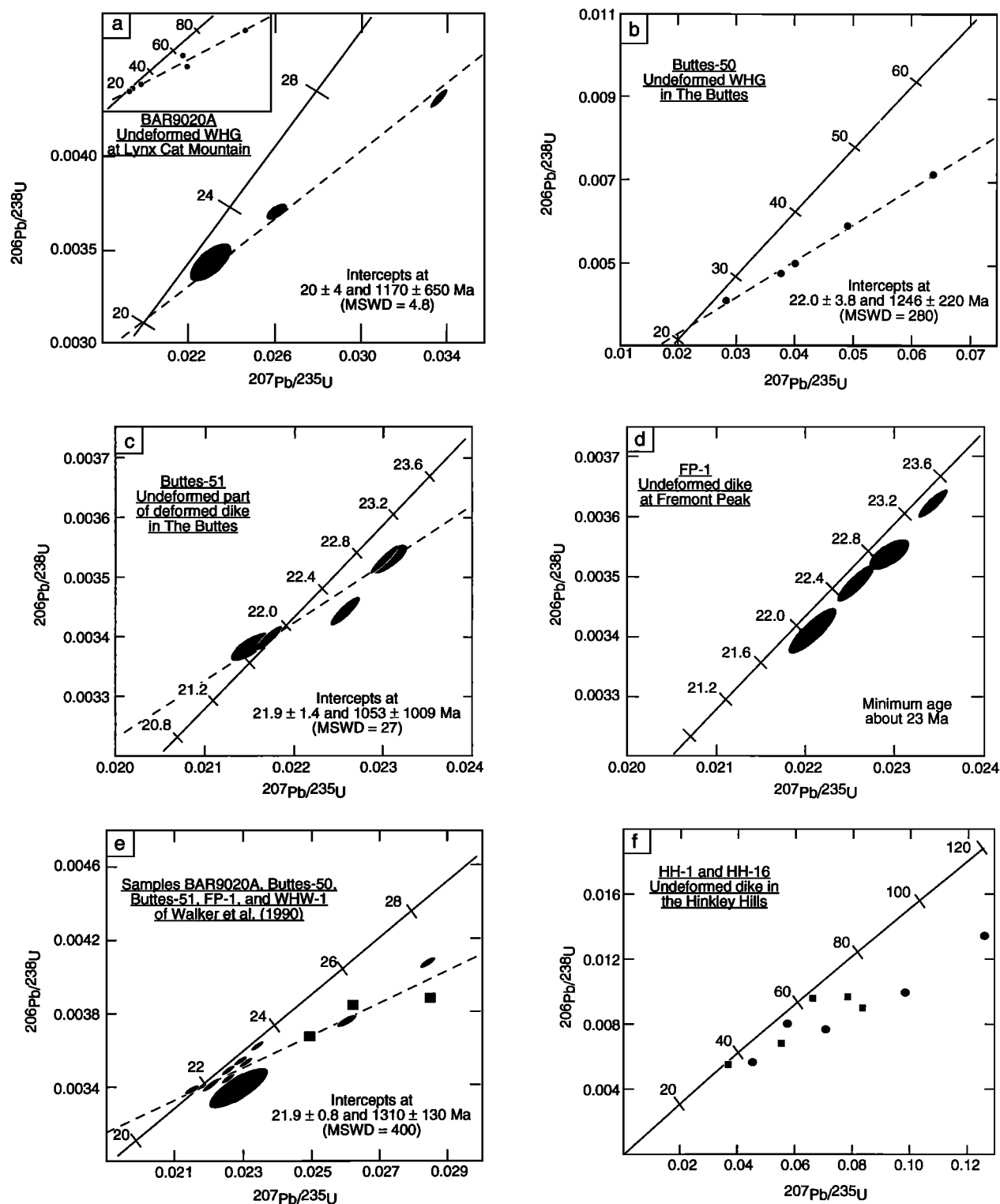


**Figure 2.** U-Pb concordia diagrams for Miocene Plutonic rocks in the central Mojave metamorphic core complex. Detailed sample locations and descriptions are given in Table 1. Analytical data are given in Table 2. (a) Sample BAR9020A, Waterman Hills granite from the Lynx Cat Mountain area. Points near concordia; inset shows all data. Data on the inset are shown as circles; see Table 2 for errors. (b) Sample Buttes-50, Waterman Hills granite from The Buttes. Data points are shown as circles; see Table 2 for errors. (c) Sample Buttes-51, dacite dike from The Buttes. (d) Sample FP-1, dacite dike from Fremont Peak. (e) Data for all of the samples and WHW-1 (squares, dacite dike in the Mitchel Range dated by Walker et al. [1990]). (f) Samples HH-1 (circles) and HH-16 (squares), dacite dikes from the Hinkley Hills.

be a Pb-loss array, and we interpret the minimum age of this sample to be around 23 Ma. Unfortunately, these fractions have high U and common Pb concentrations making interpretations somewhat uncertain.

Figure 2e shows the results from these four samples plotted together. Only the most concordant points are shown. In addition, data from sample WHW-1 from Walker *et al.* [1990] are shown as solid squares. Because all of these samples are petrographically similar (for dike and WHG suites) and apparently represent a single or short-lived intrusive event, we regressed a single discord through all of the data giving a lower intercept of  $21.9 \pm 0.8$  Ma. We interpret this to represent a mean, minimum age for the suite. It is possible that the true age is somewhat older and closer to the 23 Ma age reported for the Mitchel Range dike [Walker *et al.*, 1990]. It is possible to draw a discord between 23 Ma and 1310 Ma (mean upper intercept age) using these data: this line bounds the upper part of the data array, suggesting that most of the fractions possibly have suffered minor Pb loss. Hence our preferred interpretation for the age of the WHG intrusive event, including the pluton and associated dacitic dikes, is  $23 \pm 1$  Ma.

It is also possible that the WHG and dikes intruded and cooled over the period from 23 to 20 Ma (ages of FP-1 dikes and the BAR9020A pluton sample, respectively), and that this spread in ages represents a real variation. This may be reasonable because the dated units have variable relations to the dominant mylonitic fabric in the area. Given the possible spread in ages, intrusion and mylonitization may have occurred over a period of around 3 m.y. Unfortunately, we cannot resolve this issue fully because of the scatter in the data (which results in 1 to 4 m.y. uncertainties in the ages) and the high U concentrations (which indicates that Pb loss could be important) in these samples.

**Samples HH-1 and HH-16.** These data are from two undeformed dikes in the Hinkley Hills. Five fractions from each sample were analyzed. All fractions are discordant, and mostly show evidence of complex inherited, xenocrystic zircon. It appears that the samples contain zircon incorporated from both Mesozoic and Precambrian sources. Because of the considerable scatter in the data, no age interpretation is proposed for these samples. The data are, however, consistent with those for the other plutonic samples which indicate an early Miocene age. Hence we interpret these samples to be part of the  $23 \pm 1$  Ma suite of intrusions. This is consistent with their structural relations and overall composition.

### The $^{40}\text{Ar}/^{39}\text{Ar}$ Results

The  $^{40}\text{Ar}/^{39}\text{Ar}$  ages are used primarily to date synextensional strata in the hanging wall of the CMMCC and to correlate isolated sedimentary sequences in adjacent areas. The data set includes seven samples of tuff from the lower Pickhandle Formation in the Mud Hills, Waterman Hills, Gravel Hills, and Lead Mountain, three samples of volcanic rocks from sedimentary sequences in outlying areas, and a sample from a rhyolite plug that intrudes the Pickhandle formation in the Waterman Hills (see Table 1 for locations). Additionally, two samples of the WHG were analyzed to characterize the cooling history of the lower plate. All errors in this section are reported at the 2- $\sigma$  level.

**Pickhandle samples.** Sample MH92-1 comes from a dacite block and ash flow unit at the base of the lower Pickhandle Formation in the Mud Hills; samples MH92-2 (brown biotite-feldspar tuff) and MH92-3 (white feldspar-biotite tuff) come

from near the top of the lower Pickhandle. This is the type section of the Pickhandle Formation. A plagioclase separate from sample MH92-1 did not yield a plateau (Figure 3a and electronic supplement). Isotope correlation analysis gave a  $^{40}\text{Ar}/^{39}\text{Ar}$  intercept age of  $22.4 \pm 0.4$  Ma and a  $^{40}\text{Ar}/^{36}\text{Ar}$  intercept within error of the atmospheric value. Biotite from MH92-2 gives a flat release spectrum but no plateau. The isotope correlation diagram shows that the sample has a large radiogenic component (Figure 3b). Regression through increments 2 to 9 (containing greater than 94% of the total gas) gives an intercept age of  $21.7 \pm 0.5$  Ma and a  $^{40}\text{Ar}/^{36}\text{Ar}$  intercept well in excess of the atmospheric value. Assuming that departure from the atmospheric value is solely due to excess  $^{40}\text{Ar}$ , we accept the intercept age as the true age of this sample. Biotite from sample MH92-3 behaved similarly to MH92-2 (Figure 3c). We take the intercept age of  $21.4 \pm 0.5$  Ma to be the age of this tuff.

Sample GH-52 is a feldspar-hornblende tuff from near the base of the Pickhandle Formation in the Gravel Hills. Plagioclase from this sample did not yield a plateau, but data on an inverse isotope correlation diagram show a broad range in compositions (Figure 3d). Regression through all of the points yields an age of  $24.0 \pm 0.5$  Ma. Because increments 1, 2, and 11 fall away from the others in the release spectrum and yield little gas, an age regressed through increments 3 to 10 of  $23.8 \pm 0.5$  Ma is preferred. The  $^{40}\text{Ar}/^{36}\text{Ar}$  intercept for this is  $325 \pm 150$ . Sample WH-10 is a biotite tuff from the center part of the Pickhandle section in the upper plate of the Waterman Hills detachment fault in the Waterman Hills. This section was described in detail by Walker *et al.* [1990]. This sample yields a plateau at  $21.7 \pm 0.2$  Ma and an intercept age of  $21.7 \pm 0.5$  Ma (Figure 3e; regressed through increments 2 to 10 with a  $^{40}\text{Ar}/^{36}\text{Ar}$  intercept of  $310 \pm 70$ ). This sample is in a roughly similar stratigraphic position to MH92-2 and MH92-3.

Two samples of biotite tuff from a poorly correlated section at Lead Mountain were analyzed (Figures 3f and 3g). Biotite from sample LM-37, from the lower part of the Lead Mountain sections, gives no plateau. Regression through increments 2 to 10 on an inverse isotope correlation diagram gives an intercept age of  $23.0 \pm 0.5$  Ma and a  $^{40}\text{Ar}/^{36}\text{Ar}$  intercept of  $350 \pm 80$ . This is interpreted to be the eruptive age of the sample. Biotite from LM-38, a stratigraphically higher sample in a similar position to samples WH-10, MH92-2, and MH92-3, is better behaved and gives a plateau age of  $23.6 \pm 0.2$  Ma (Figure 3g). The inverse isotope correlation diagram shows a relatively restricted range of compositions. Regression through increments 2 to 9 (containing greater than 97% of the gas) gives an intercept age of  $21.3 \pm 0.5$  Ma and a  $^{40}\text{Ar}/^{36}\text{Ar}$  intercept well in excess of the atmospheric value. We assume that the difference from the atmospheric value is due to excess  $^{40}\text{Ar}$  and accept the intercept age as the true age of the sample.

**Other volcanic samples.** Other samples were obtained for regional comparison (Table 1 and electronic supplement and Figure 4). Two samples come from the Box Canyon area of the Rodman Mountains. Biotite from BOXC-26 yields a largely concordant spectrum with a plateau age of  $24.0 \pm 0.4$  Ma (Figure 4a). An inverse isotope correlation diagram shows a  $^{40}\text{Ar}/^{36}\text{Ar}$  intercept at the atmospheric value and an intercept age of  $24.4 \pm 0.3$  Ma. We take the mean of these ages,  $24.2 \pm 0.4$  Ma, to be the best estimate for the age of the sample. Plagioclase from ROD3.19 gave a saddle-shaped spectrum (Figure 4b). On an inverse isotope correlation diagram, the  $^{40}\text{Ar}/^{36}\text{Ar}$  intercept is above the atmospheric value, and the intercept age is  $23.1 \pm 0.6$  Ma. This is interpreted as the age of this sample. The spectrum and the  $^{40}\text{Ar}/^{36}\text{Ar}$  inter-

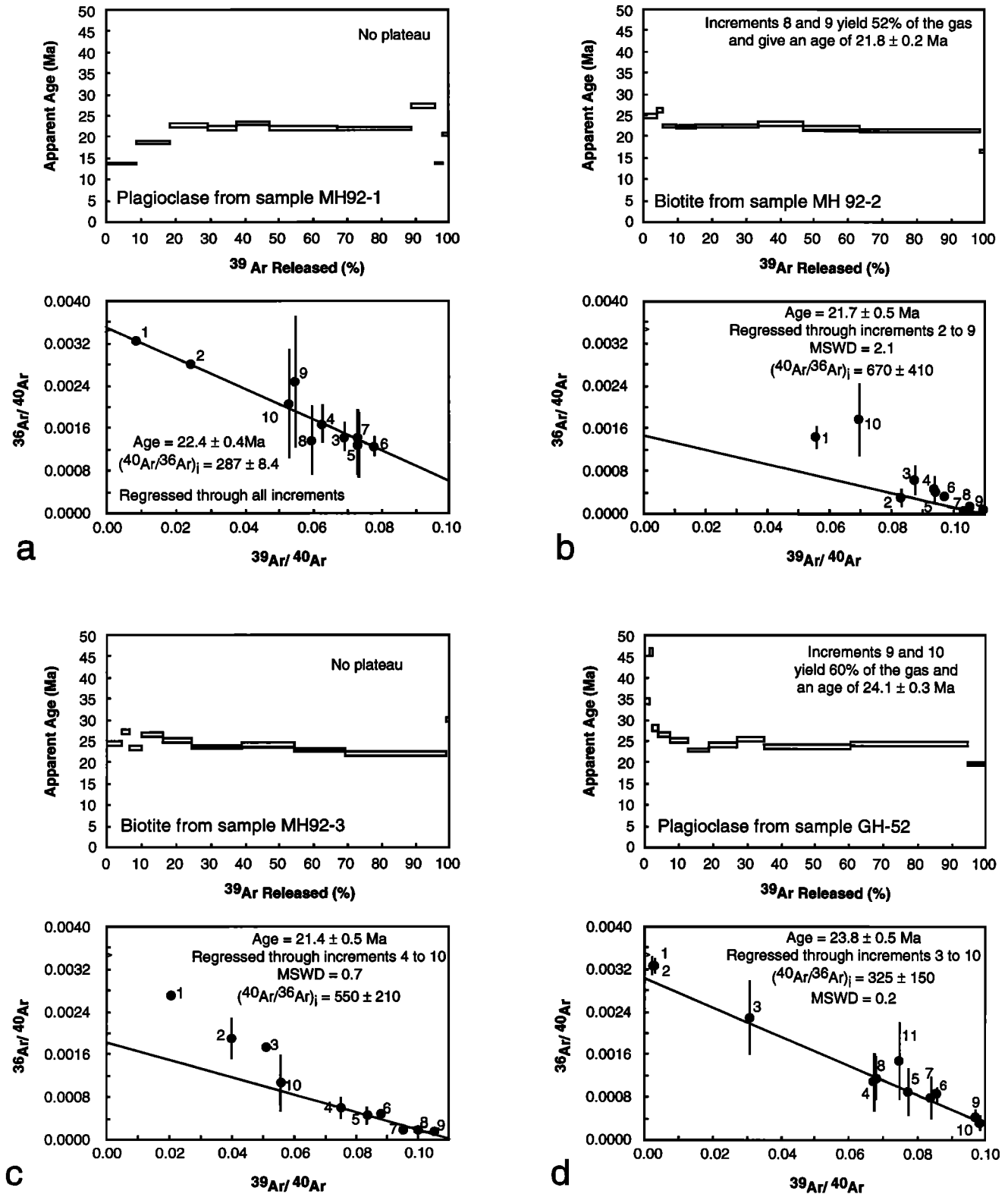


**Figure 3.** The  $^{40}\text{Ar}/^{39}\text{Ar}$  age data for Pickhandle Formation. Detailed sample locations and descriptions are given in Table 1. Analytical data are given in electronic supplement. (a) Sample MH92-1, dacite tuff in basal part of the Pickhandle Formation in the Mud Hills. (b) Sample MH92-2, crystal tuff in the middle of the Pickhandle Formation in the Mud Hills. (c) Sample MH92-3, feldspar-biotite tuff in the middle of the Pickhandle Formation in the Mud Hills. Sample is stratigraphically above MH92-2. (d) Sample GH-52, tuff in the lower Pickhandle Formation in the Gravel Hills. (e) Sample WH-10, pumiceous tuff in the middle part of the Pickhandle Formation in the Waterman Hills. (f) Sample LM-37, pumiceous biotite tuff at Lead Mountain. (g) Sample LM-38, white biotite tuff at Lead Mountain.

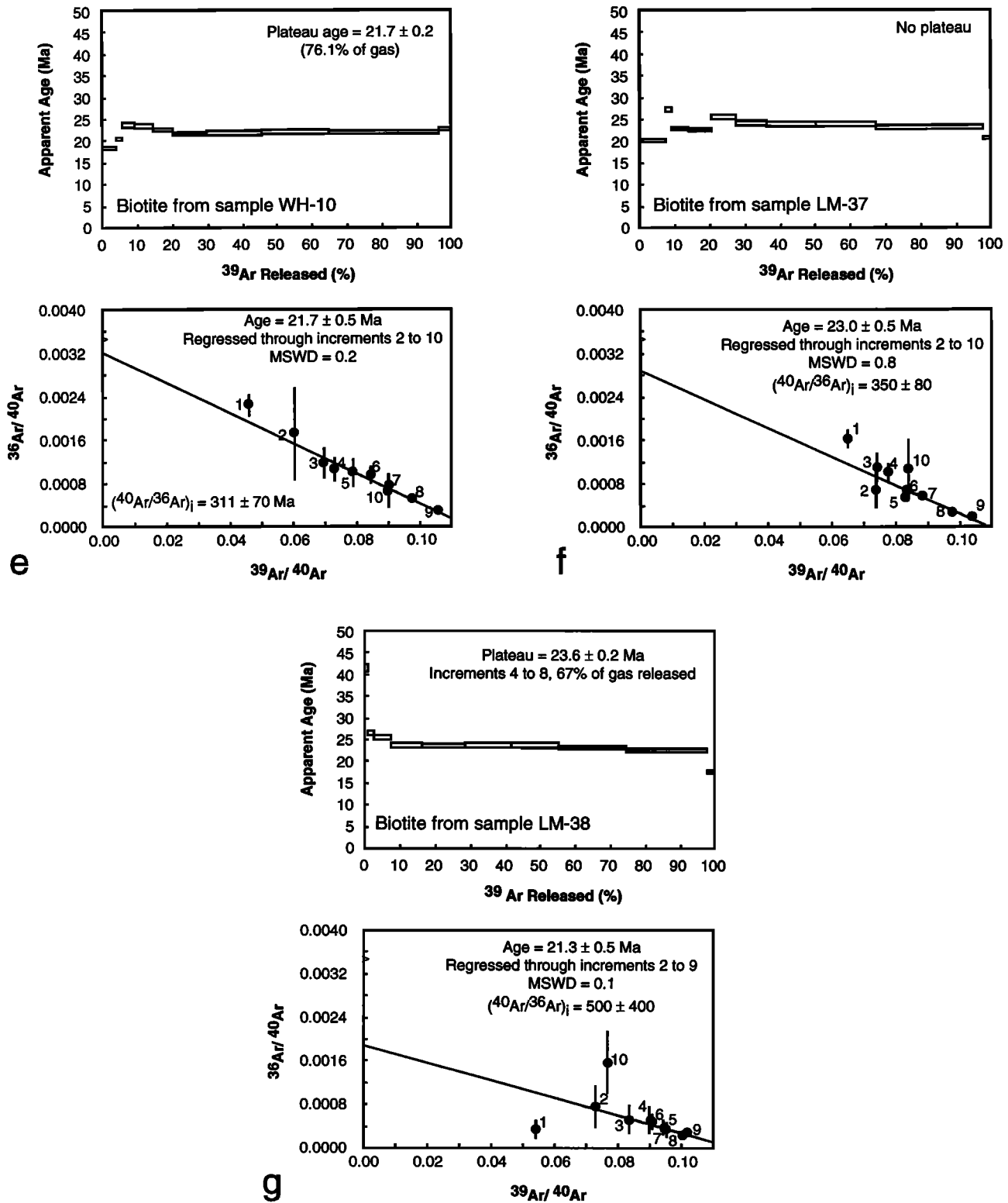


Figure 3. (continued)

cept indicate that excess  $^{40}\text{Ar}$  is probably present and that the lowest point in the saddle of the spectrum is a maximum age for this sample. This age,  $23.1 \pm 0.5$  Ma, is consistent with the intercept age.

A sample of tuff from the Lenwood anticline, sample BARS-B, was also analyzed (Figure 4c). This sample did not yield a plateau but gives an intercept age of  $21.8 \pm 0.5$  Ma and a

$^{40}\text{Ar}/^{36}\text{Ar}$  intercept above the atmospheric value. This age is interpreted as the best estimate of the age of the rock. Hence, this sample correlates with the Pickhandle Formation.

**Upper plate intrusive rocks.** We have also obtained an age on biotite from a rhyolite plug in the Waterman Hills which intrudes the Pickhandle Formation and is cut by the brittle detachment fault (sample WHG-14). This plug may be part of a

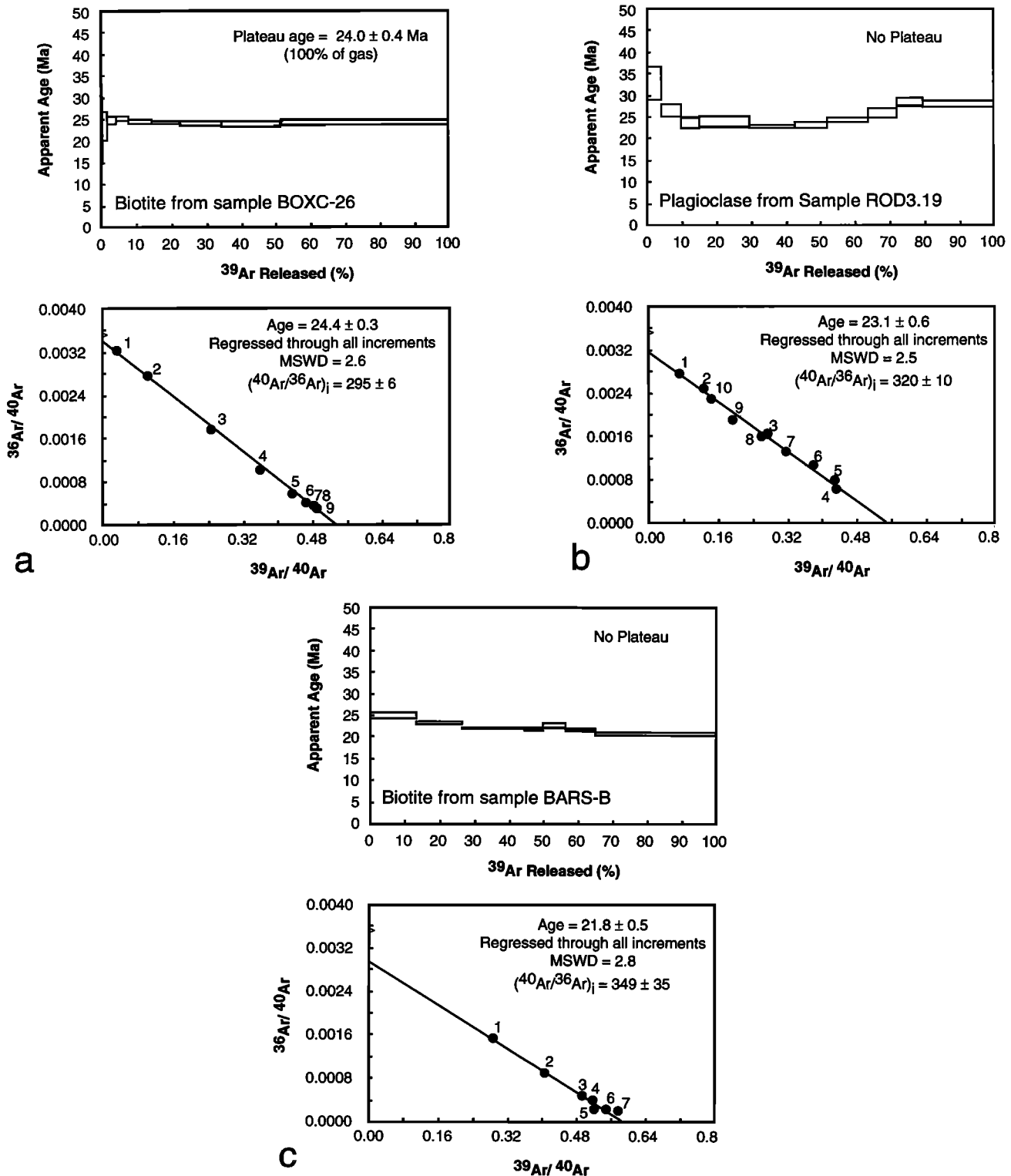


**Figure 4.** The  $^{40}\text{Ar}/^{39}\text{Ar}$  age data for volcanic rocks south of the CMMCC. Detailed sample locations and descriptions are given in Table 1. Analytical data are given in the electronic supplement. (a) Sample BOXC-26, plagioclase-biotite tuff from the Box Canyon area of the Rodman Mountain. (b) Sample ROD3.19, lithic airfall tuff in Silver Bell Canyon in the Rodman Mountains. (c) Sample BARS-B, white tuff exposed in the Lenwood anticline.

widespread suite of rhyolite intrusions around the Barstow area [Dibblee, 1967]. The sample does not yield a plateau, but gives an intercept age of  $20.0 \pm 0.3$  Ma (Figure 5a). It does, however, give a  $^{40}\text{Ar}/^{36}\text{Ar}$  intercept below atmospheric, indicating some nonsystematic behavior. Although the cause of this variation

from the atmospheric value is uncertain, it could result from inaccuracies of the blank corrections to measured data. We propose, however, the 20 Ma date as a fair estimate of the age of this sample: this sample is from a shallowly intruded plug that probably cooled quickly.

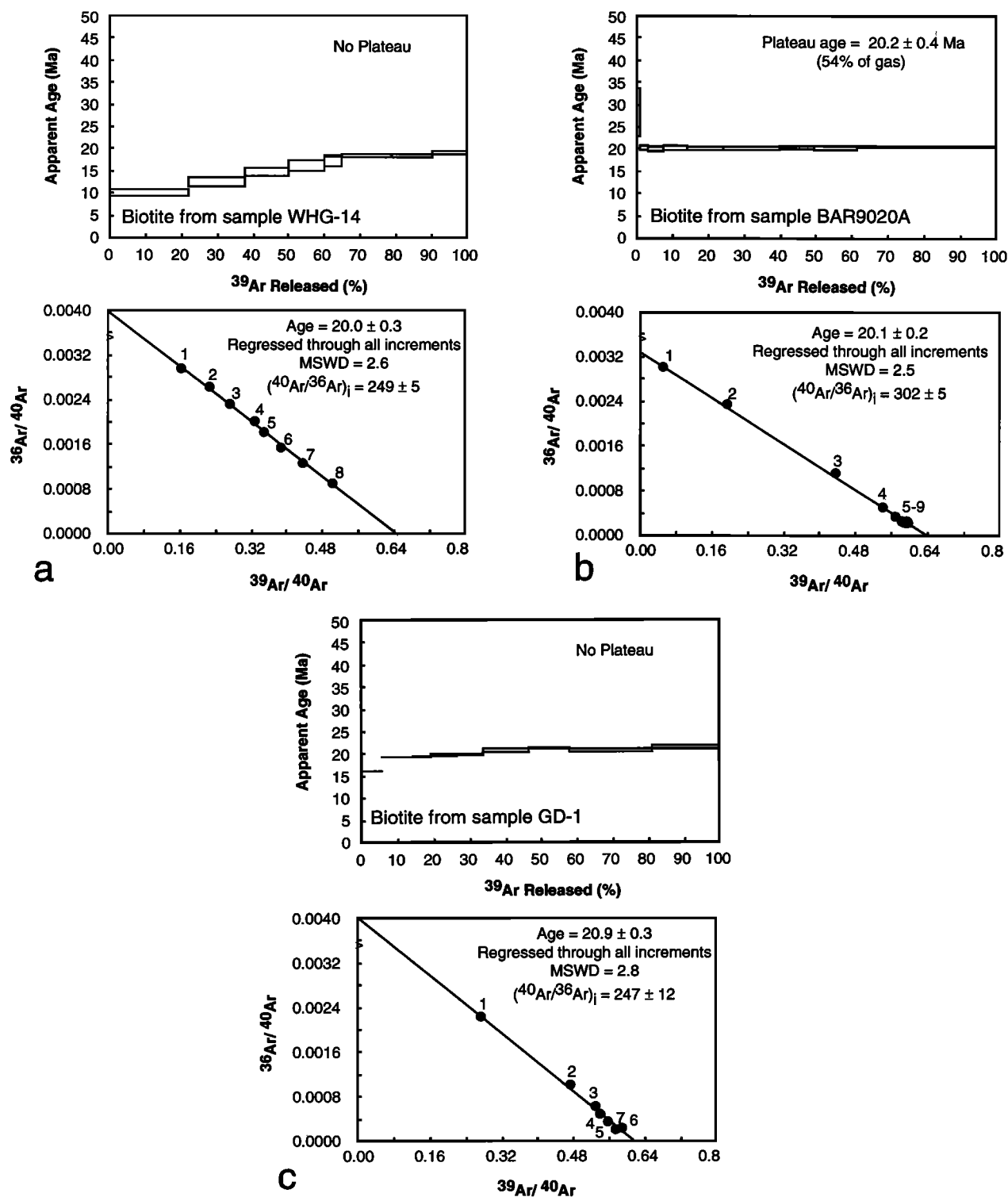


**Figure 5.** The  $^{40}\text{Ar}/^{39}\text{Ar}$  age data for plutonic rocks in the CMMCC. Detailed sample locations and descriptions are given in Table 1. Analytical data are given in the electronic supplement. (a) Sample WHG14, rhyolite plug cutting the Pickhandle Formation but cut by the Waterman Hills detachment fault in the Waterman Hills. (b) Sample BAR9020A, Waterman Hills granite from Lynx Cat Mountain. (c) Sample GD-1, Waterman Hills granite from the Waterman Hills.

**Lower plate plutonic rocks.** We also obtained two cooling ages on biotite from the WHG (electronic supplement and Figure 5). Sample BAR9020A is from the same sample that we obtained a zircon age of  $20 \pm 4$  Ma. This sample yields a plateau age of  $20.1 \pm 0.3$  Ma and an intercept age of  $20.1 \pm 0.2$  Ma

(Figure 5b). Hence we interpret this sample to have cooled through biotite closure at  $20.1 \pm 0.2$  Ma. Sample GD-1 is WHG in the Waterman Hills. It does not yield a plateau but gives an intercept age of  $20.9 \pm 0.3$  Ma (Figure 5c). This sample also yields a  $^{40}\text{Ar}/^{36}\text{Ar}$  intercept below atmospheric, indicating some

nonsystematic behavior possibly due to inaccuracies of the blank corrections. We interpret these ages as the time that the samples BAR9020A and GD-1 cooled through  $\sim 300^{\circ}\text{C}$ .

## Discussion

The geochronologic results described above can be combined with field relations to gain a better understanding of the CMMCC and the connection between magmatism, extension, and mylonitization. Below, we discuss the implications of these new data for regional stratigraphic development, the intrusive history of the area and its connection to volcanism, and the overall structural and magmatic development of the CMMCC.

### Regional Correlation of the Pickhandle Formation

The strata dated from the Waterman Hills and Gravel Hills areas had been previously correlated with the type Pickhandle Formation in the Mud Hills [Dibblee, 1968; Fillmore and Walker, 1993, 1995; Walker *et al.*, 1990]. The ages determined in this study support this correlation and show that the Lower Pickhandle Formation was deposited between  $\sim 24$  and 21.3 Ma and the upper Pickhandle Formation was deposited between 21.3 and 19 Ma (lower age limit obtained in this study and the upper age limit based on the age of the overlying Barstow Formation from Woodburne *et al.* [1990]). In addition, rocks exposed in the Lenwood anticline are at least in part early Miocene in age and coeval with the Pickhandle Formation.

Two tuffs from the sequence at Lead Mountain yield ages ( $23.0 \pm 0.5$  Ma and  $21.7 \pm 0.5$  Ma) that are younger than the ages of intrusive phases that presumably cut the strata as reported by Dokka and Woodburne [1986] and Lambert *et al.* [1987] (e.g., both 25.6 Ma). Our ages are consistent with the age (21.0 Ma) of a presumably crosscutting intrusion published by Dokka *et al.* [1991]. However, because the actual data and sample locations were never reported in those studies, we cannot evaluate the discrepancy, and the differences between samples and/or methods resulting in the 25.6 versus 21.0 Ma ages were not discussed by Dokka *et al.* [1991]. Fillmore and Walker [1995] considered the Lead Mountain rocks to be correlative to the Pickhandle Formation based on sedimentological and stratigraphic criteria, and this interpretation is consistent with the ages reported here. Additionally, the upper unit dated at 21.3 Ma is in roughly the same position in the Pickhandle stratigraphy as similar age rocks in the Mud Hills and Waterman Hills [Fillmore and Walker, 1995].

The 23–24 Ma ages for volcanic rocks in the Rodman Mountains area suggest that basin development there was initiated before or during rifting in the CMMCC. However, the age of ROD3.19 shows that most of the volcanism in this southern area occurred prior to deposition of the Pickhandle Formation in the CMMCC (the sample lies stratigraphically above  $\sim 2$  km of volcanic flows, Table 1).

### Development of the Pickhandle Basin

Before discussing the Pickhandle basin in detail, we must address the possibilities of large-scale crustal rotations in this part of the Mojave Desert. Dokka [1989] considered the CMMCC and its associated fabrics to have undergone about  $45^{\circ}$  of clockwise rotation based on his interpretation of paleomagnetic results. Recent results by Valentine *et al.* [1993] for rocks in the study area show a more complex picture; Jackhammer Formation strata show a  $55^{\circ}$  clockwise declination anomaly, and Pickhandle strata

show a  $23^{\circ}$  counterclockwise declination anomaly. Because we have shown above that the Pickhandle is coeval with the formation of the mylonitic fabrics, the results of Valentine *et al.* [1993] could be taken to indicate that the footwall fabrics should be restored in a clockwise rather than counterclockwise manner. The results from the Pickhandle Formation, however, are not regionally uniform: Pickhandle in the Calico Mountains seems to show no declination anomaly. This indicates to us that any rotations are local rather than regional in importance.

We accept here the interpretations of Bartley and Glazner [1991] and Valentine *et al.* [1993] that the observed rotations, if real, affect only rocks above the regional detachment and are not rooted through the entire crust. This means that although there may be some local rotation of hanging wall strata, the overall arrangement of facies trends and other features are not rotated in a bulk sense in the CMMCC. This is most consistent with important regional features, as pointed out by Bartley and Glazner [1991]: first, the Independence dike swarm is regionally consistent in orientation, despite being exposed in several areas of putative large rotations; and second, the extension direction between the coeval CMMCC and the Colorado River extensional corridor is consistent in orientation and to the northeast. Hence we discuss the development of the Pickhandle basin using present-day geographic coordinates as reference.

The Pickhandle basin initiated at  $\sim 24$  Ma as a northwest trending trough bounded to the southwest by the breakaway of the CMMCC and to the northeast by the hanging wall of the extensional system [Fillmore and Walker, 1995]. The dominant sediment source for the lower Pickhandle Formation was an intrabasinal volcanic center that shed detritus to the southeast and northwest. The distribution of proximal through distal facies suggests that the volcanic center may have been located in the Calico Mountains (Figure 1).

During deposition of the upper Pickhandle Formation ( $\sim 21.3$  to 19.0 Ma), volcanism waned and the elongate basin was partitioned into two subbasins: one to the southeast that includes the Waterman Hills and Lead Mountain area, and one to the northwest that includes the Mud Hills and Gravel Hills areas (Figure 1 [Fillmore and Walker, 1995]). Paleogeographic reconstruction of these basins, based on provenance determinations and facies distribution, suggests that the southeast subbasin had internal drainage with a large lacustrine system situated in the depocenter. The northwestern margin of the lake was bounded by a south flowing fluvial system that drained highlands composed of Paleozoic metasedimentary and Mesozoic plutonic rocks. The southeastern margin was fringed by a northward prograding alluvial fan system that drained a source of the Mesozoic volcanic and plutonic rocks. On the basis of the offset of its source terrane, Fillmore and Walker [1995] interpreted this fan system to have drained the escarpment of a right-lateral transfer fault that marked the southeastern margin of the main Pickhandle basin and the CMMCC. A similar southwest striking transfer fault was proposed by Martin *et al.* [1993], based on the offset of pre-Tertiary tectonic elements. This inferred fault is required to accommodate differential extension between the CMMCC to the north and the less extended areas to the south. Ages for the Box Canyon area determined in this study indicate that volcanism and basin development apparently began somewhat earlier in this southern area.

We are uncertain whether to include rocks in the Daggett Ridge and Newberry Mountains in this basin. Rocks in these areas are of the same age as the Pickhandle Formation [Dokka, 1986, 1989] and are lithologically quite similar. However, in

contrast to the CMMCC where displacement of the synextensional strata is large, extension in the Newberry Mountains smaller in magnitude [Dokka, 1989; Bartley and Glazner, 1991]. In addition, a major transform structure seems to be present between the CMMCC and the Newberry Mountains [Dokka, 1989; Martin *et al.*, 1993; Fillmore and Walker, 1995]. Hence we lump these strata into the Pickhandle Group (Figure 1) but consider them to have been deposited in a basin isolated from the main CMMCC.

The age of the hanging wall rhyolite plug in the Waterman Hills (WHG-14) indicates that brittle detachment faulting continued to at least 20 Ma. This is consistent with the footwall cooling ages reported in this study. On the basis of the age of this plug, hanging wall strata in the Waterman Hills [Walker *et al.*, 1990] were folded between about 21.7 and 20 Ma.

### Relations Between Magma Emplacement and Extension

There has been much interest in the connection of magmatism with extensional deformation [e.g., Gans *et al.*, 1989; Lister and Baldwin, 1993]. Magmatism and deformation can strongly influence each other. In a metamorphic core complex setting, there are a number of different ways that deformation can induce the generation and migration of magma. Footwall rocks can undergo rapid isothermal decompression which may generate melt. In addition, deformation can create dilatant openings as a result of rock failure and strain incompatibilities. On the other hand, magmatism can induce deformation and rock failure through a number of mechanisms. Thermal weakening can greatly enhance deformation [e.g., Hollister and Crawford, 1986]. In a nonhydrostatic stress field magma bodies and plutons can increase and reorient the principal stresses around their margins which may lead to rock failure [e.g. Parsons and Thompson, 1993].

Each of these processes predicts a specific sequence of events that should be recorded in the relative timing of deformation and magmatism. If extension leads to the generation of melts, then plutonic bodies will probably postdate most of the footwall mylonitic fabrics. This will also be the case if faulting opens cracks to be filled by synextensional magmas (e.g., dike swarms in extensional settings). Alternatively, if heat advected by magmas leads to thermal weakening, then intrusion and mylonitization should be intimately associated.

Field relationships, mostly from the footwall of the core complex, suggest that some of these processes may have operated in the CMMCC. The Hinkley Hills are cut by numerous dikes that were largely emplaced after mylonitization. This suggests that extension created space for dike intrusion mainly through brittle failure. In the Mitchel Range and Waterman Hills, dikes and plutons were emplaced both prekinematically and synkinematically, and thus deformation and magmatism may have had mutually enhancing affects; that is, magmatism may have thermally weakened the crust and dilatant openings in the deforming crust may have enhanced magma migration.

In The Buttes, strain is localized in dikes and their wall rocks at the outcrop scale which suggests thermal weakening. Dikes in this region, however, are typically thin, about 1-2 m wide, and the thermal pulse may be too short-lived to greatly enhance deformation other than in areas within a few meters of the dikes. In the Fremont Peak (footwall) and Lead Mountain (hanging wall) areas, dike swarms intrude rocks that record little or no ductile deformation, and thus there seems to be no direct local relationship between magmatism and mylonitization.

Although the relation of magmatism to extension is clear locally for the CMMCC, the overall connection is somewhat un-

certain. Some authors have suggested that heat input to the crust from magmatism triggers extensional deformation [e.g., Gans *et al.*, 1989]. In the CMMCC, however, it is clear that prekinematic intrusion and volcanism are minor. Mylonitic deformation apparently began prior to emplacement of the main body of the WHG [Fletcher and Bartley, 1994], and only small dikes are clearly prekinematic to early kinematic. Hence a triggering mechanism for extension in which large amounts of heat are advected into the crust with sufficient time for the crust to adjust thermally and fail seems unlikely for the CMMCC. Effects should be much more local than regional in scope considering the essentially coincident timing between plutonism and extension.

It is clear, however, that the CMMCC is situated at the locus of early Miocene magmatism. Mylonitic footwall rocks are everywhere spatially associated with Miocene intrusions. In addition, the boundaries of the CMMCC seem to correspond, in a general way, with the limits of the magmatism (both plutonism and volcanism). These boundaries are defined on the presence of the Pickhandle basin, extent of mylonitic rocks, and the distribution of areas showing evidence for extensional deformation (Figure 1). Southward, basement rocks are not cut by voluminous Miocene intrusive rocks [Dibblee, 1964, 1966, 1967, 1970; Dokka, 1986, 1989; Glazner *et al.*, 1994] and extension was transferred to areas to the east and south [Bartley and Glazner, 1991; Martin *et al.*, 1993]. Likewise, early Miocene igneous rocks are not exposed north of Fremont Peak [Dibblee, 1968; Glazner *et al.*, 1994], and extension must somehow have been transferred to areas east or west of the Fremont Peak area.

These relationships suggest that perhaps both magmatism and extensional deformation were localized by some larger-scale lithospheric process. It is possible that the CMMCC lies between two right-stepping right-lateral faults which may have localized both extensional deformation and magmatism. In this view, the CMMCC would occupy a releasing bend position between the Mojave Valley fault to the southeast [Bartley and Glazner, 1991; Martin *et al.*, 1993] and an inferred transfer fault to the northwest (Figure 6). The breakaway for the CMMCC probably does not continue northward, because synextensional strata and footwall fabrics are not present in the Lava Mountains [Smith, 1964; Fillmore and Walker, 1995]. The location of the inferred fault is uncertain, but it would probably be located south of the Rand Mountains: when motion along the Garlock fault is restored, rocks in the Rand Mountains lie adjacent to similar rocks in the Tehachapi Mountains. This implies to us that the probable position for the transfer fault is the gap between Fremont Peak and the Rand Mountains. It is unlikely that the extension transferred to the northeast into the Death Valley region, because structures of early Miocene age are poorly represented in that area. It may continue westward into the Tehachapi Mountains and southern San Joaquin Valley where Goodman and Malin [1992] suggested that there may be early Miocene extension. It is also possible that the Mojave extension dies out into the Tehachapi/San Joaquin area resulting in the observed clockwise rotations of lower Miocene strata and basement rocks [Kanter and McWilliams, 1982].

### Conclusions

1. Igneous activity and extensional deformation in the CMMCC are intimately associated in time and space. However, any single direct cause-and-effect relationship between the two seems implausible.

2. The dominant extension-related intrusive phase is an early Miocene granite that was previously unrecognized in the central



**Figure 6.** Transfer fault model for the development of the CMMCC. The Waterman Hills detachment fault, the main low-angle normal fault in the CMMCC is shown by bold lines north of Barstow. Miocene sedimentary rocks above the Waterman Hills detachment fault are shown with a diagonal rule. Miocene plutonic rocks in the footwall of the detachment are shown with random dash pattern. The main separation between hanging wall and footwall rocks is shown by bold line with tic marks (on upper plate). Position of the transfer structures are only broadly constrained. Miocene rocks in the Newberry Mountains are age equivalent to the Pickhandle Group: these rocks are south of the Mojave Valley fault (main transfer structure) but are internally somewhat extended. For this reason a splay of the Waterman Hills detachment is drawn into this area.

Mojave Desert. Intrusive phases in the footwall of the CMMCC define a rather small range of ages. The U/Pb data from all footwall samples define a single discord that has a lower intercept of  $21.9 \pm 0.8$  Ma and give a preferred age of  $23 \pm 1$  Ma.

3. Volcanic rocks deposited in the rift basins are coeval with footwall intrusive rocks and appear to be similar in composition. Therefore, in the CMMCC, footwall intrusion may represent the sources of the volcanic rocks deposited in the synextensional basins.

4. The age of extensional deformation in the CMMCC is indicated by the nearly continuous record of rift-related sedimentary rocks of the Pickhandle Formation. The lower Pickhandle Formation was deposited between  $\sim 24$  and 21.3 Ma, and the upper Pickhandle Formation was deposited between 21.3 and 19 Ma.

5. Strata that can be broadly correlated by age with the Pickhandle are also exposed in the Lenwood anticline and at

Lead Mountain. Rocks in the Box Canyon area of the Rodman Mountains are probably slightly older than the Pickhandle Formation. This indicates that volcanism and basin development south of the CMMCC began slightly earlier.

**Acknowledgments.** Financial support for this project was provided by National Science Foundation grants EAR-8816944 and EAR-8916838 to Bartley, EAR-8817076 and EAR-8917291 to Glazner, and EAR-8816628 and EAR-8916802 to Walker. Support was also provided by a Sigma Xi research grant (1989) and a Shell Oil Graduate Fellowship awarded (1990-1991) to Martin, and by the Petroleum Research Fund, administered by the American Chemical Society. We thank Kip Hodges and Dan Lux for use of laboratories needed for this study, and for comments on sections of this manuscript. We thank Randy Van Schmus and Drew Coleman for looking over the U-Pb sections of this paper and Clark Isachsen for providing a copy of his program PB MACDAT for data reduction and plotting. Discussions with Jonathan Miller were quite valuable to the outcome of this paper. John Bendixen assisted in mapping and

collecting geochronology samples. We also thank JGR reviewers Brad Hacker and Greg Davis and associate editors Rod Metcalf and Gene Smith for comments that greatly improved this manuscript.

## References

- Alexander, E. C., Jr., G. M. Mickelson, and M. A. Lanphere, MMhb-1: A new  $^{40}\text{Ar}/^{39}\text{Ar}$  dating standard, *U.S. Geol. Surv. Open File Rep.*, 78-701, 6-8, 1978.
- Anderson, J. L., A. P. Barth, and E. D. Young, Mid-crustal roots of Cordilleran metamorphic core complexes, *Geology*, 16, 366-369, 1988.
- Bartley, J. M., and A. F. Glazner, En echelon Miocene rifting in the southwestern United States and model for vertical-axis rotation in continental extension, *Geology*, 19, 1165-1168, 1991.
- Bartley, J. M., J. M. Fletcher, and A. F. Glazner, Tertiary extension and contraction of lower-plate rocks in the central Mojave metamorphic core complex, southern California, *Tectonics*, 9, 521-534, 1990.
- Beratan, K. K., Miocene synextensional sedimentation patterns, Whipple Mountains, southeastern California: Implications for the geometry of the Whipple detachment system, *J. Geophys. Res.*, 96, 12,425-12,442, 1991.
- Burke, D. B., J. W. Hillhouse, E. H. McKee, S. T. Miller, and J. L. Morton, Cenozoic rocks in the Barstow basin area of southern California-Stratigraphic relations, radiometric ages, and paleomagnetism, *U.S. Geol. Surv. Bull.*, 1529-E, 16 pp., 1982.
- Cebula, G. T., M. J. Kunk, H. H. Mehnert, C. W. Naeser, J. D. Obradovich, and J. F. Sutter, The Fish Canyon Tuff, a potential standard for the  $^{40}\text{Ar}$ - $^{39}\text{Ar}$  and fission track methods, *Terra Cognita*, 6, 139-140, 1986.
- Coney, P. J., Cordilleran metamorphic core complexes: An overview, in *Cordilleran Metamorphic Core Complexes*, edited by M. D. Crittenden Jr., P. J. Coney, and G. H. Davis, pp. 7-31, Geological Society of America, Boulder, Colo., 1980.
- Crittenden, M. D., Jr., Metamorphic core complexes of the North American Cordillera: Summary, in *Cordilleran Metamorphic Core Complexes*, edited by M. D. Crittenden Jr., P. J. Coney, and G. H. Davis, pp. 485-490, Geological Society of America, Boulder, Colo., 1980.
- Dibblee, T. W., Jr., Geologic map of the Rodman Mountains quadrangle, San Bernardino County, California, scale 1:62,500, *U.S. Geol. Surv. Map*, I-430, 1964.
- Dibblee, T. W., Jr., Geologic map of the Newberry quadrangle, San Bernardino County, California, scale 1:62,500, *U.S. Geol. Surv. Map*, I-461, 1966.
- Dibblee, T. W., Jr., Areal geology of the western Mojave Desert, California, *U.S. Geol. Surv. Prof. Pap.* 522, 153 pp., 1967.
- Dibblee, T. W., Jr., Geology of the Fremont Peak and Opal Mountain quadrangles, California, *Calif. Div. of Mines Geol. Bull.*, 188, 64 pp., 1968.
- Dibblee, T. W., Jr., Geologic map of the Daggett quadrangle, San Bernardino County, California, scale 1:62,500, *U.S. Geol. Surv. Map*, I-592, 1970.
- Dickinson, W. R., Tectonic setting of faulted Tertiary strata associated with the Catalina core complex in southern Arizona, *Spec. Pap. Geol. Soc. Am.*, 264, 106 pp., 1991.
- Dokka, R. K., Patterns and modes of early Miocene crustal extension, central Mojave Desert, California, in *Spec. Pap. Geol. Soc. Am.*, 208, pp. 75-95, 1986.
- Dokka, R. K., The Mojave extensional belt of southern California, *Tectonics*, 8, 363-390, 1989.
- Dokka, R. K., and A. K. Baksi, Thermochronology of detachment faults of the Mojave extensional belt, California: A progress report, *Geol. Soc. Am. Abstr. Programs*, 20, A16, 1988.
- Dokka, R. K., and M. O. Woodburne, Mid-Tertiary extensional tectonics and sedimentation, central Mojave Desert, California, *LSU Publ. Geol. Geophys. Tectonics Sediment.*, 1, 55 pp., 1986.
- Dokka, R. K., M. McCurry, M. O. Woodburne, E. G. Frost, and D. A. Okaya, A field guide to the Cenozoic structure of the Mojave Desert, in *This Extended Land - Geological Journeys in the Southern Basin and Range*, edited by D. L. Weide and M. L. Faber, pp. 21-49, University of Nevada, Las Vegas, 1988.
- Dokka, R. K., D. J. Henry, T. M. Ross, A. K. Baksi, J. Lambert, C. J. Travis, S. M. Jones, C. J. Jacobson, M. M. McCurry, M. O. Woodburne, and J. P. Ford, Aspects of the Mesozoic and Cenozoic geologic evolution of the Mojave Desert, in *Geological Excursions in Southern California and Mexico, Geological Society of America Annual Meeting Guidebook*, pp. 1-43, Department of Geological Sciences, San Diego State University, San Diego, Calif., 1991.
- Duebendorfer, E. M., and E. T. Wallin, Basin development and syntectonic sedimentation associated with kinematically coupled strike-slip and detachment faulting, southern Nevada, *Geology*, 19, 87-90, 1991.
- Fedo, C. M., and J. M. G. Miller, Evolution of a Miocene half-graben basin, Colorado River extensional corridor, southeastern California, *Geol. Soc. Am. Bull.*, 104, 481-493, 1992.
- Fillmore, R. P., and J. D. Walker, Three extensional basin types associated with detachment-style faulting, early Miocene of the central Mojave Desert, *Geol. Soc. Am. Abstr. Programs*, 25, 37, 1993.
- Fillmore, R. P., and J. D. Walker, The early Miocene Pickhandle basin, central Mojave Desert, California, *Spec. Pap. Geol. Soc. Am.*, in press, 1995.
- Fletcher, J. M., Geodynamics of large-magnitude extension: A field based study of the central Mojave metamorphic core complex, Ph.D. dissertation, 109 pp., Univ. of Utah, Salt Lake, 1994.
- Fletcher, J. M., and J. M. Bartley, Constrictional strain in a non-coaxial shear zone: Implications for fold and rock fabric development, central Mojave metamorphic core complex, California, *J. Struct. Geol.*, 16, 555-570, 1994.
- Gans, P. B., G. A. Mahood, and E. Schermer, Synextensional magmatism in the Basin and Range Province; A case study from the eastern Great Basin, *Spec. Pap. Geol. Soc. Am.*, 233, 53 pp., 1989.
- Glazner, A. F., J. M. Bartley, and J. D. Walker, Geology of the Waterman Hills detachment fault, central Mojave Desert, California, in *This Extended Land - Geological Surveys in the Southern Basin and Range*, edited by D. L. Weide and M. L. Faber, pp. 225-237, University of Nevada, Las Vegas, 1988.
- Glazner, A. F., J. M. Bartley, and J. D. Walker, Magnitude and significance of Miocene crustal extension in the central Mojave Desert, California, *Geology*, 17, 50-54, 1989.
- Glazner, A. F., J. M. Fletcher, J. M. Bartley, J. D. Walker, M. W. Martin, J. S. Miller, W. J. Taylor, D. S. Coleman, Widespread Miocene plutonism and ductile deformation in the central Mojave metamorphic core complex, California, *Eos Trans. AGU*, 73(43), (abstract), Fall Meeting suppl., 548, 1992.
- Glazner, A. F., J. D. Walker, J. M. Bartley, J. M. Fletcher, M. W. Martin, E. R. Schermer, S. S. Boettcher, J. S. Miller, R. P. Fillmore, and J. K. Linn, Reconstruction of the Mojave Block, in *Geological Investigations of an Active Margin*, edited by S. F. McGill and T. M. Ross, pp. 3-30, San Diego County Museum Association, Redlands, Calif., 1994.
- Goodman, E. D., and P. E. Malin, Evolution of the southern San Joaquin basin and mid-Tertiary "transitional" tectonics, central California, *Tectonics*, 11, 478-498, 1992.
- Hodges, K. V., W. E. Hames, W. Olszewski, B. C. Burchfiel, L. H. Royden, and Z. Chen, Thermobarometric and  $^{40}\text{Ar}/^{39}\text{Ar}$  geochronologic constraints on Eohimalayan metamorphism in the Dinggyê area, southern Tibet, *Contrib. Mineral. Petrol.*, 117, 151-163, 1994.
- Hollister, L. S., and M. L. Crawford, Melt-enhanced deformation: A major tectonic process. *Geology*, 14, 558-561, 1986.
- Hubacher, F., and D. R. Lux, Timing of Acadian deformation in north-eastern Maine, *Geology*, 15, 80-83, 1987.
- Kanter, L. R., and M. O. McWilliams, Rotation of the southernmost Sierra Nevada, California, *J. Geophys. Res.*, 87, 3819-3830, 1983.
- Krogh, T. E., A low contamination method for hydrothermal decomposition of zircon and extraction of U and Pb for isotopic age determinations, *Geochim. Cosmochim. Acta*, 37, 485-494, 1973.

- Krogh, T. E., Improved accuracy of U-Pb zircon ages by the creation of more concordant systems using air abrasion technique, *Geochim. Cosmochim. Acta*, **46**, 637-649, 1982.
- Lambert, J. R., R. K. Dokka, and A. K. Baksi, Lead Mountain caldera complex: earliest Tertiary magmatism in the central Mojave Desert, California, *Geol. Soc. Am. Abstr. Programs*, **19**, 738, 1987.
- Lister, G. S., and S. L. Baldwin, Plutonism and the origin of metamorphic core complexes, *Geology*, **21**, 607-610, 1993.
- Ludwig, K. R., Calculation of uncertainties of U-Pb data, *Earth Planet. Sci. Lett.*, **46**, 212-220, 1980.
- MacFadden, B. J., C.C. Swisher, N. D. Opdyke, and M. O. Woodburne, Paleomagnetism, geochronology, and possible tectonic rotation of the middle Miocene Barstow Formation, Mojave Desert, southern California, *Geol. Soc. Am. Bull.*, **102**, 478-493, 1990.
- Martin, M. W., A. F. Glazner, J. D. Walker, and E. R. Schermer, Evidence for right-lateral transfer faulting accommodating an echelon Miocene extension, Mojave Desert, California, *Geology*, **21**, 355-358, 1993.
- McCulloh, T.H., Geology of the southern half of the Lane Mountain Quadrangle, California, Ph.D. thesis, 180 pp., Univ. of Calif., Los Angeles, 1952.
- McCulloh, T.H., Geologic map of the Lane Mountain Quadrangle, California, scale 1:48,000, *U. S. Geol. Surv. Open File Map*, 1960.
- Nielson, J. E., and K. K. Beratan, Tertiary basin development and tectonic implications, Whipple detachment system, Colorado River extensional corridor, California and Arizona, *J. Geophys. Res.*, **95**, 599-614, 1990.
- Parrish, R. R., An improved micro-capsule for zircon dissolution in U-Pb geochronology, *Chem. Geol.*, **66**, 99-102, 1987.
- Parsons, T., and G. A. Thompson, Does magmatism influence low-angle normal faulting, *Geology*, **21**, 247-250, 1993.
- Reynolds, S. J., and W. A. Rehrig, Mid-Tertiary plutonism and mylonitization, South Mountains, central Arizona, in *Cordilleran Metamorphic Core Complexes*, edited by M. D. Crittenden Jr., P. J. Coney, and G. H. Davis, pp. 159-175, Geological Society of America, Boulder, Colo., 1980.
- Reynolds, S. J., J. E. Spencer, S. M. Richard, and S. E. Laubach, Mesozoic structures in west-central Arizona, *Ariz. Geol. Soc. Dig.*, **16**, 35-51, 1986.
- Roddick, J. C., W. D. Loweridge, and R. R. Parrish, Precise U/Pb dating of zircon at the sub-nanogram Pb level, *Chem. Geol.*, **66**, 111-121, 1987.
- Samson, S. D., and E. C. Alexander, Calibration of the interlaboratory  $^{40}\text{Ar}/^{39}\text{Ar}$  dating standard, MMhb-1, *Chem. Geol.*, **66**, 27-34, 1987.
- Smith, G. I., Geology and volcanic petrology of the Lava Mountains, San Bernardino County, California, *U.S. Geol. Surv. Prof. Pap.*, **457**, 97 pp., 1964.
- Stacey, J. S., and J. D. Kramers, Approximation of terrestrial lead isotope evolution by a two-stage model, *Earth Planet. Sci. Lett.*, **26**, 207-221, 1975.
- Steiger, R. H., and E. Jäger, Convention on the use of decay constants in geo- and cosmochemistry, *Earth Planet. Sci. Lett.*, **36**, 359-362, 1977.
- Valentine, M. J., L. L. Brown, and M. P. Golombek, Cenozoic crustal rotations in the Mojave Desert from paleomagnetic studies around Barstow, California, *Tectonics*, **12**, 666-677, 1993.
- Walker, J. D., J. M. Bartley, and A. F. Glazner, Large-Magnitude Miocene Extension in the Central Mojave Desert: Implications for Paleozoic to Tertiary Paleogeography and Tectonics, *J. Geophys. Res.*, **95**, 557-569, 1990.
- Woodburne, M. O., R. H. Tedford, and C. C. I. Swisher, Lithostratigraphy, biostratigraphy, and geochronology of the Barstow Formation, Mojave Desert, southern California, *Geol. Soc. Am. Bull.*, **102**, 459-477, 1990.

---

J. M. Bartley, 717 Browning Building, Department of Geology and Geophysics, University of Utah, Salt Lake City, UT 84112-1183. (e-mail: jmbartle@cc.utah.edu).

Robert P. Fillmore, Department of Geology, Northern Arizona University, Flagstaff, AZ, 86011-6030.

John M. Fletcher, Departamento de Geologia, CICESE, P.O. Box 434843, San Ysidro, CA, 91243-4843. (e-mail: jfletche@cicese.mx).

Allen F. Glazner, Department of Geology, CB 3315, Mitchell Hall, University of North Carolina, Chapel Hill, Chapel Hill, NC 27599-3315. (e-mail: afg@unc.edu).

Mark W. Martin, Servicio Nacional de Geología y Minería-Chile, Avda. Santa María 0104, Casilla 1347, Santiago, Chile. (e-mail: sermageo@huelen.reuna.cl).

Wanda J. Taylor, Department of Geoscience, University of Nevada, Las Vegas, 4505 Maryland Parkway, Las Vegas, NV 89154-4010. (e-mail: wjt@nevada.edu).

J. Douglas Walker, Isotope Geochemistry Laboratory and Department of Geology, 2291 Irving Hill Drive, University of Kansas, Lawrence, KS 66045-2969. (e-mail: jdwalker@kuhub.cc.ukans.edu).

(Received May 26, 1994; revised October 17, 1994;  
accepted November 29, 1994.)